Progress in Natural Science: Materials International 2013;23(2):170–173

Chinese Materials Research Society

Progress in Natural Science: Materials International

www.elsevier.com/locate/pnsmi
www.sciencedirect.com

ORIGINAL RESEARCH

Boron nitride nanotube reinforced polyurethane composites

Luhua Li[a,*], Ying Chen[a], Zbigniew H. Stachurski[b]

[a]*Institute for Frontier Materials, Deakin University, Geelong Waurn Ponds Campus, Waurn Ponds, Victoria 3216, Australia*
[b]*Research School of Engineering, College of Engineering and Computer Science, The Australian National University, Canberra, ACT 0200, Australia*

Received 29 October 2012; accepted 26 January 2013
Available online 11 April 2013

KEYWORDS

Composite;
Boron nitride nanotube;
Compressive modulus;
Rockwell hardness

Abstract Bulk-sized boron nitride nanotube (BNNT) reinforced polyurethane (PU) composites at different volume contents have been produced. A large quantity of BNNT fillers are synthesized by a boron ink method. Compared to the neat PU, the 0.5 vol% and 2.0 vol% BNNT reinforced composites show 38.2% and 6.3% increases in compressive modulus, respectively. The relatively less enhanced compressive modulus of the 2.0 vol% composite may be due to the agglomerations of nanotubes at high volume percentages. Contrary to normal behaviour, the composites show decreasing Rockwell (HRR) hardness values with an increasing volume fraction.

1. Introduction

Boron nitride nanotubes (BNNTs) have many interesting properties. In contrast to carbon nanotubes (CNTs) which are zero or narrow bandgap materials, BNNTs have a bandgap of ~6 eV regardless of diameter or chirality change. BNNTs are promising deep ultraviolet light emitters suitable for laser and optoelectronics [1]. BNNTs have superb stiffness and bending flexibility along the axial direction with Young's modulus of 1.22 TPa, thanks to the tubular structure and the strong sp^2 bonding [2]. This value is in the same range as the measured Young's modulus of CNTs, but almost one order of magnitude higher than that of other known insulating fibres. The plastic deformation of BNNTs under axial compression is anisotropic due to the relative radial displacements of B and N atoms. BNNTs have a thermodynamic yield limit higher than CNTs under constant strain or in a high temperature environment. BNNTs have better thermal and chemical stabilities than CNTs: CNTs are oxidized at 400–500 °C in air and totally burnt out at ~700 °C; by contrast, the oxidation of BNNTs starts at 650–950 °C and the burning-out happens above 1200 °C [3]. The thermal conductivity of BNNTs is of the same order as that of CNTs due to the same phonon dispersion relation, although hexagonal boron nitride (*h*BN) has a lower thermal conductivity than graphite. It is worth noting that BNNTs exhibit the biggest

*Corresponding author. Tel.: +61 3 5227 2589.
E-mail address: luhua.li@deakin.edu.au (L. Li).

Peer review under responsibility of Chinese Materials Research Society.

ELSEVIER Production and hosting by Elsevier

http://dx.doi.org/10.1016/j.pnsc.2013.03.004

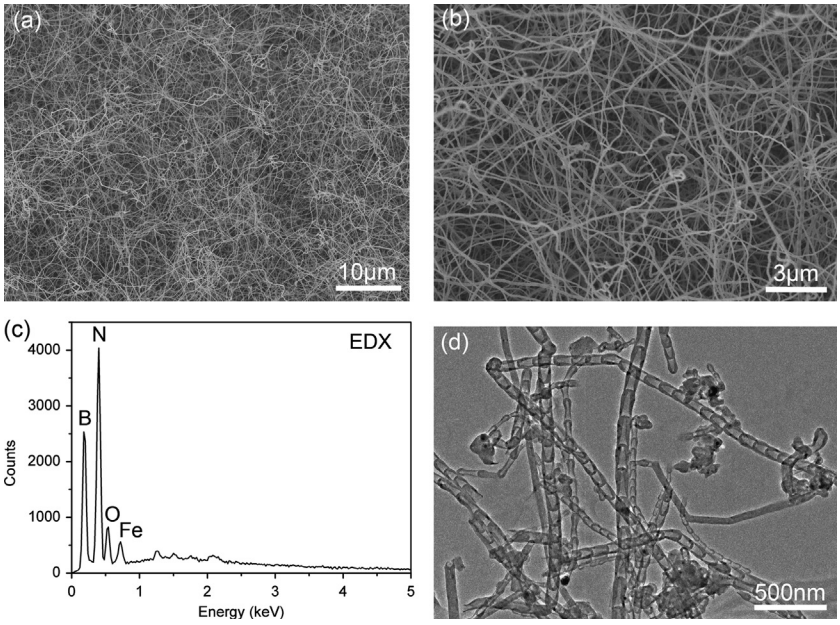

Fig. 1 (a),(b) SEM images; (c) EDX spectrum; and (d) TEM image of the BNNTs used for composite production.

thermal conductivity boost of any known material from changes in isotopic content. BNNTs with more than 99.5% ^{11}B can have a thermal isotope effect of about 50% [4], which gives rise to an even better thermal conductivity than most CNTs. BNNTs show lower cytotoxicity than CNTs and are more suitable for bioapplications [5].

BNNTs have been used in the production of nanocomposites. Polymeric composites, such as polystyrene (PS) [6], polymethyl methacrylate (PMMA) [7], polyvinyl alcohol (PVA), and polylactide–polycaprolactone copolymer [8], reinforced by BNNTs have been prepared. BNNTs are better candidates for ceramic matrix composite due to their higher thermal stability. Alumina (Al_2O_3) [9], silicon nitride (Si_3N_4) [10], barium calcium aluminosilicate glass [11] BNNT ceramic composites have been reported. There have also been attempts to use BNNTs in metal composites [12]. The improvements of mechanical performances have been achieved in these composites, demonstrating that BNNTs are effective in composite applications.

In this study, BNNTs were added to polyurethane (PU), one of the most frequently used polymers, at different volume percentages to produce bulk sized (not film) composites. Mechanical properties, including compressive modulus and hardness, of the composites were measured. The microstructures of the composite were investigated by scanning electron microscopy (SEM) to understand the changes of mechanical properties.

2. Experimental

The BNNTs were produced by the boron ink method [13,14]. Amorphous B powder of 2 g (95–97%, Sigma-Aldrich) was sealed in a steel milling vial with four hardened steel balls with a diameter of 25.4 mm. Anhydrous ammonia (NH_3) at a static pressure of 300 kPa was purged into the milling vial prior to the milling treatment. The rolling ball milling was carried out for 150 h at a rotation speed of 155 rpm. B ink was prepared by mixing the ball milled B particles with ferric nitrate (98%, Sigma-Aldrich) in ethanol solution under 0.5 h ultrasonic bath. The additional nitrate can greatly enhance the yield of BNNTs [15]. The ink-like solution was then poured into a crucible and isothermally annealed using a horizontal tube furnace at 1100 °C for 3 h in nitrogen plus 15% hydrogen (N_2+15% H_2) at a gas flow rate of 0.1 L/min. After annealing, BNNTs were harvested.

A neat PU and two BNNT reinforced PU composites at 0.5 vol % and 2 vol% were prepared. For the composites, 0.20 g and 0.77 g BNNTs were dispersed in acetone (6.25 g, Merck AR grade) for 2 h under ultrasonic bath. A bench-top ultrasonicator (Model 28x, Neytech) was used at 80 W power. Fifteen grams of polyurethane prepolymer (TGI-PPG prepolymer, Airthane PPT-80A, Air Products and Chemicals) was dissolved in each of the BNNT acetone solutions. Magnetic stirring at 40 °C homogeneously mixed the BNNT with the prepolymer and eliminated the acetone solvent via evaporation. Next, 3.75 g of hardener (aromatic diamine, Lonzacure MCDEA-GS, Air Products and Chemicals) was melted at 95 °C and poured into each of the prepolymers containing BNNTs. Further stirring was conducted in vacuum to mix the prepolymer with the hardener and remove any entrained air. The mixtures were moved into cylindrical moulds and held for 24 h in vacuum (~10^{-1} mbar) at room temperature. All the samples were pre-cured at 40 °C in air for 8 h and post-cured at 100 °C in air for 15 h. The final cylindrical composites had a diameter of 31.5 mm and heights of 16–20 mm. The neat PU sample was produced at the same time following a similar procedure without BNNTs.

Samples were analysed using the following methods. Nanotube phases were investigated using a Philips 3020 X-ray diffraction (XRD) machine. A Hitachi 4300SE/N SEM at 3 kV was employed to examine the morphologies of nanotube and composite. The elemental composition of the nanotubes was measured using an X-ray energy dispersive spectroscopy (EDS) attached to the SEM. Transmission electron microscope (TEM) investigations were performed using a JEOL 2100F instrument. The Rockwell hardness was measured at various locations on the polished composite surfaces with a 1/2 inch diameter steel sphere under 60 kg load (HRR). The hardness values were averaged from at least five measurements at different locations. The compression tests were

conducted on an Instron 5500R1186 machine at 28 °C and 22% humidity. The crosshead speed was 2 mm/min and the maximum load was ~2 kN.

3. Results and discussion

A high-yield boron ink method was used to produce BNNT fillers for composite [13,14]. Figs. 1a and b show the SEM images of the BNNTs produced by the ink method. The EDS spectrum in Fig. 1c confirms that the product is dominated by B and N elements, along with a small amount of O and Fe. The Fe comes from both the steel particles derived from the repeated collision between milling balls and vial, as well as the Fe decomposed from the added Fe $(NO_3)_3$. The TEM image in Fig. 1d discloses that most of the nanotubes have a bamboo-like structure and diameters of 40–80 nm. A small amount of cylindrical BNNTs are also encountered during the TEM investigations. The BNNT products were added to PU after 2 h sonication bath in acetone.

Compared to the neat PU, the two composites with 0.5 vol% and 2 vol% of BNNTs have higher compressive moduli. Fig. 2 compares the compressive stress–strain curves of the three samples. The compressive moduli of the neat PU and the 0.5 vol% BNNT reinforced composites are 19.8 MPa and 27.4 MPa, respectively. Compared to the neat PU, the 0.5 vol% BNNT filled composite shows a 38.2% enhancement of compressive modulus. SEM investigations (Fig. 3a and b) on several fracture surfaces of the composite revealed that the 0.5 vol% BNNT composite, as a whole, had a good dispersion of nanotubes, though some agglomerations were also found. This may be because of the relatively low volume percentage of nanotubes used, the small attractions among the relatively large nanotubes and the impacts from sonication. The sonication of the BNNTs in solvent could not only separate BNNTs but also shorten the bamboo structured BNNTs [16]. The shortened BNNTs have a much lower chance of bundling during composite

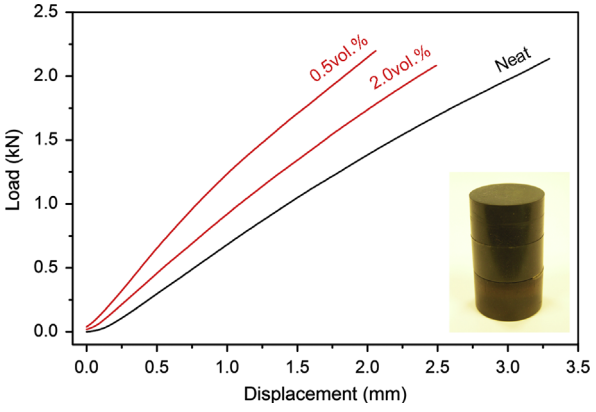

Fig. 2 Compressive stress–strain curves of neat PU, 0.5 vol% and 2.0 vol% BNNT reinforced PU composites. The inset shows a digital photo of the neat PU (bottom), 0.5 vol% PU composite (middle) and 2.0 vol% PU composite (top).

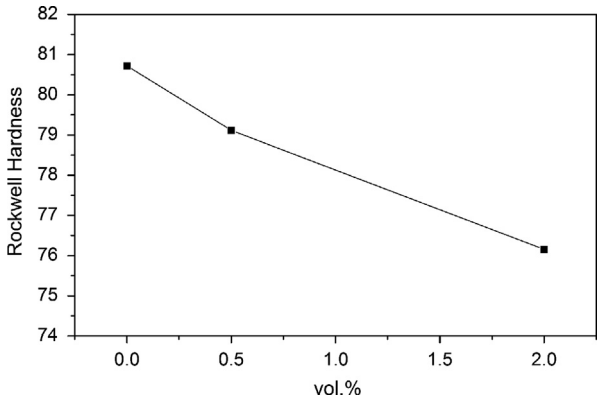

Fig. 4 HRR hardness values of neat PU, 0.5 vol% and 2.0 vol% BNNT reinforced PU composites.

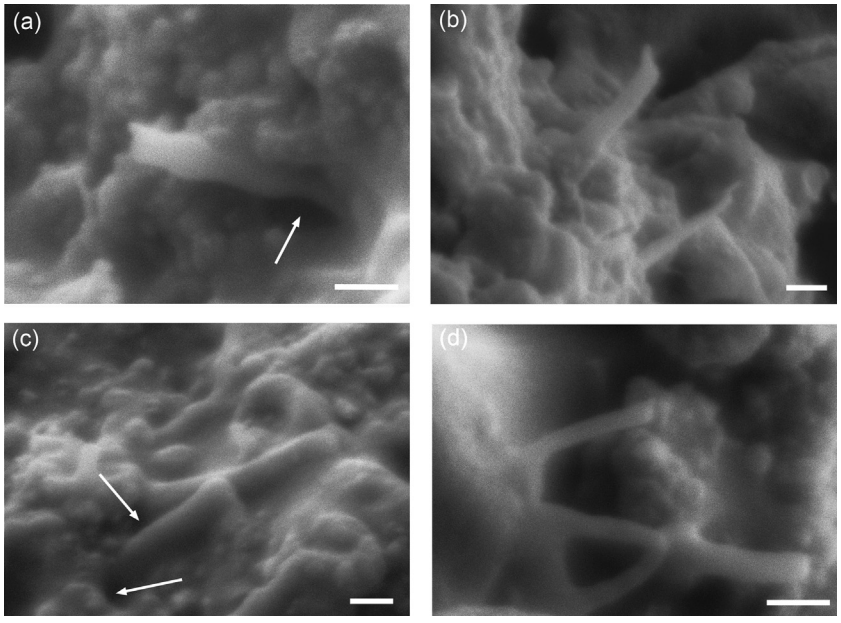

Fig. 3 SEM images of (a) and (b) the fractured surface of 0.5 vol% composite, with a void arrowed; (c) and (d) the fractured surface of 2.0 vol% composite, where more agglomeration of BNNTs can be seen. Two voids are arrowed in (c). All scale bars are 200 nm.

preparation. The surface tension of individual BNNTs was measured to be 26.7 mN/m [17] and the calculated dispersive and polar components of the surface tension of BNNTs are $\gamma^{d}=22.5$ mN/m and $\gamma^{p}=4.3$ mN/m respectively [18]. These values are quite similar to those of CNTs, but much larger than those of *h*BN, mainly because the positive Laplace pressure introduced by high surface curvature and nanoscale size can exceed the adhering disjoining pressure and cause the water film on the cylindrical surface to become unstable [18]. These results suggest that good adhesion to matrix is more difficult to be achieved on BNNTs than *h*BN particles in composite. SEM observations of the fractured composite surface revealed the adhesion between BNNTs and PU. It showed that most BNNTs tended to break rather than pull out (Fig. 3a and b). This suggests that the binding between BNNTs and the polymer matrix was strong enough to transfer the load from the matrix to the nanotubes so that the mechanical enhancement was obtained. Both the large diameter and the geometrical shape of the bamboo BNNTs [19] may have contributed to mechanical interlocking or non-covalent bonding between nanotubes and matrix. However, sometimes there are observable voids between BNNTs and the polymer matrix (Fig. 3a, arrowed).

The 2 vol% BNNT reinforced composite exhibited a lower compressive modulus value of 21.1 MPa. This decline is mainly caused by the agglomeration of nanotubes. As the volume content of nanotubes in the matrix increases, the chance of agglomeration increases dramatically due to the large surface area of nanotubes. These agglomerates can cause voids and adhesion defects in the composite. The SEM images in Fig. 3c and d show examples of voids and defects due to the agglomerations of BNNTs. During fracture, the crack propagated along the interface between two nanotubes and polymer as well as the voids caused by the crossing of the two tubes.

The hardness of the composite decreased with increasing BNNT content. The neat PU had a Rockwell hardness of 80.7 ± 2.1 HRR, while the 0.5 vol% and 2 vol% BNNT reinforced PU composites had 79.1 ± 1.9 HRR and 76.2 ± 4.2 HRR, respectively (Fig. 4). Rockwell hardness involves pressing a steel ball (the indenter) into the flat surface of a sample. The difference in depth between the initial position at pre-load, and the final position at full load, is taken as the hardness number. The deformation will likely have three components: (i) elastic (Hertzian), (ii) brittle (Griffiths), and (iii) ductile (Huber–von Mises). For a fibre reinforced composite the extent of each component will depend on the applied load as well as the volume fraction of the reinforcing phase. Since the fibres are much stiffer and stronger than the matrix, one should expect the hardness to increase with fibre content under the condition of perfect adhesion and no defects [20]. In fact, the opposite is observed in our composites, as shown in Fig. 4. This is most probably due to the number of voids in the composite samples that increases with increasing nanotube content. This trend is also consistent with more agglomerates in the 2 vol% BNNT reinforced composite.

4. Conclusion

Bulk sized BNNT reinforced PU composites at different volume contents were prepared. The BNNTs were produced by the B ink method. The 0.5 vol% and 2.0 vol% BNNT reinforced composites showed 38.2% and 6.3% increases in compressive modulus respectively compared to the neat PU. The relatively decreased compressive modulus of 2.0 vol% composite may be due to the agglomerations of nanotubes at high volume percentage. The composites showed slightly smaller HRR hardness because of the presence of voids.

Acknowledgement

L.H. Li thanks the assistance received from Dr. Peter Lamb from Deakin University during the manuscript preparation.

References

[1] L.H. Li, Y. Chen, M.Y. Lin, et al., Single deep ultraviolet light emission from boron nitride nanotube film, Applied Physics Letters 97 (2010) 141104-1–141104-4.
[2] N.G. Chopra, A. Zettl, Measurement of the elastic modulus of a multi-wall boron nitride nanotube, Solid State Communications 105 (1998) 297–300.
[3] Y. Chen, J. Zou, S.J. Campbell, et al., Boron nitride nanotubes: pronounced resistance to oxidation, Applied Physics Letters 84 (2004) 2430–2432.
[4] C.W. Chang, A.M. Fennimore, A. Afanasiev, et al., Isotope effect on the thermal conductivity of boron nitride nanotubes, Physical Review Letters 97 (2006) 085901.
[5] L. Li, L.H. Li, S. Ramakrishnan, et al., Controlling wettability of boron nitride nanotube films and improved cell proliferation, Journal of Physical Chemistry C 116 (2012) 18334–18339.
[6] C.Y. Zhi, Y. Bando, C.C. Tang, et al., Boron nitride nanotubes/polystyrene composites, Journal of Materials Research 21 (2006) 2794–2800.
[7] C.Y. Zhi, Y. Bando, W.L.L. Wang, et al., Mechanical and thermal properties of polymethyl methacrylate–BN nanotube composites, Journal of Nanomaterials 2008 (2008) 642036.
[8] D. Lahiri, F. Rouzaud, T. Richard, et al., Boron nitride nanotube reinforced polylactide–polycaprolactone copolymer composite: mechanical properties and cytocompatibility with osteoblasts and macrophages in vitro, Acta Biomaterialia 6 (2010) 3524–3533.
[9] L.A. Xue, I.W. Chen, Superplastic alumina at temperatures below 1300 °C using charge-compensating dopants, Journal of the American Ceramic Society 79 (1996) 233–238.
[10] Q. Huang, Y.S. Bando, X. Xu, et al., Enhancing superplasticity of engineering ceramics by introducing BN nanotubes, Nanotechnology 18 (2007) 485706.
[11] N.P. Bansal, J.B. Hurst, S.R. Choi, Boron nitride nanotubes-reinforced glass composites, Journal of the American Ceramic Society 89 (2006) 388–390.
[12] D. Lahiri, V. Singh, L.H. Li, et al., Insight into reactions and interface between boron nitride nanotube and aluminum, Journal of Materials Research 27 (2012) 2760–2770.
[13] L.H. Li, Y. Chen, A.M. Glushenkov, Synthesis of boron nitride nanotubes by boron ink annealing, Nanotechnology 21 (2010) 105601.
[14] L.H. Li, Y. Chen, A.M. Glushenkov, Boron nitride nanotube films grown from boron ink painting, Journal of Materials Chemistry 20 (2010) 9679–9683.
[15] L. Li, L. Li, Y. Chen, et al., Mechanically activated catalyst mixing for high-yield boron nitride nanotube growth, Nanoscale Research Letters 7 (2012) 417.
[16] Y. Yu, H. Chen, Y. Liu, et al., Preparation and potential application of boron nitride nanocups, Materials Letters 80 (2012) 148–151.
[17] K. Yum, M.F. Yu, Measurement of wetting properties of individual boron nitride nanotubes with the Wilhelmy method using a nanotube-based force sensor, Nano Letters 6 (2006) 329–333.
[18] L.H. Li, Y. Chen, Superhydrophobic properties of nonaligned boron nitride nanotube films, Langmuir 26 (2010) 5135–5140.
[19] M. Olek, J. Ostrander, S. Jurga, et al., Layer-by-layer assembled composites from multiwall carbon nanotubes with different morphologies, Nano Letters 4 (2004) 1889–1895.
[20] A. Hodzic, J.K. Kim, Z.H. Stachurski, Nano-indentation and nano-scratch of polymer/glass interfaces, II: model of interphases in water aged composite materials, Polymer 42 (2001) 5701–5710.